

ELECTROMAGNETIC STRUCTURE OF NUCLEI*

R. G. ARNOLD

*The American University, Washington, D.C. 20016**and**Stanford Linear Accelerator Center, Stanford, CA 94305***ABSTRACT**

A brief review is given of selected topics in the electromagnetic structure of nucleons and nuclei for which significant progress was obtained in the two years since the last meeting in this series at Steamboat Springs Colorado.

INTRODUCTION

Electromagnetic probes of nucleon and nuclear targets continues to provide crucial information for understanding the internal structure of hadronic matter. The experimental and theoretical progress in the last two years has extended our understanding in several key areas. On the experimental side, new results have been obtained in part because high current electron beams in the GeV energy range are now available for nuclear scattering experiments. On the theoretical side there is much activity trying to formulate a consistent picture of nucleon and nuclear structure including quark degrees of freedom. This task is far from complete, but we can report progress in the following areas.

NUCLEON FORM FACTORS

We know from much evidence that nucleons are extended composite particles that participate in the strong, electromagnetic, and weak interactions. Measurements of the e.m. form factors

$$G_E = F_1 - \frac{Q^2}{4m^2} F_2 \quad (1.a)$$

$$G_M = F_1 + F_2 \quad (1.b)$$

where F_1 and F_2 are the Dirac and Pauli form factors, gives information about the distribution of charge and current in the nucleons and about the nature of the virtual photon-nucleon interaction. At low energy the data are interpreted to give charge and current distributions, but the constituents are not resolved. In the GeV energy range the vector meson dominance model (VMD)¹ pictures the interaction of the virtual photon with the nucleon to be composed of two

* Work supported in part by the Department of Energy, contract DE-AC03-76F00515 (SLAC) and by the National Science Foundation, Grant PHY85-10549 (American University).

parts: interaction of a bare photon, and interaction of the hadronic (vector meson) components of the virtual photon. At higher energy the hadronic VMD interaction is expected to give way to hard scattering from the nucleon quark constituents described^{2,4} by perturbative QCD (PQCD). A central question today is: Where is perturbative QCD applicable? There are new experimental and theoretical results bearing on that question.

Form Factors in Perturbative QCD

The hadron electromagnetic form factors are calculated^{2,4} in PQCD as a special case of exclusive reactions (kinematics of all initial and final particles specified). The amplitude for scattering is predicted to factorize into a product of a hard scattering amplitude, containing the pointlike interaction of n valence quarks, times a probability amplitude for finding the n quarks in the initial and final wave functions. The hard scattering is governed by the laws of QCD with quark-gluon coupling given by $\alpha_S(Q^2)$. The quark wave functions for color singlet hadrons can be written as a sum of components starting with the lowest n quark valence component and summing over higher states containing extra quarks and gluons (ocean components). The form factors are predicted^{2,3} to have power law falloff at large Q^2

$$F(Q^2) \simeq \left(\frac{1}{Q^2}\right)^{n-1}. \quad (2)$$

The contributions from the non-valence quarks decrease faster with increasing Q^2 due to the penalty for transferring momentum to extra constituents. The quark helicity is conserved in the interactions of the vector photon with massless spin one-half quarks.⁵ This leads to the suppression of the Pauli (spin flip) terms compared to the Dirac terms by an extra power of $1/Q^2$

$$F_1 \simeq \frac{C_1}{Q^4}; \quad F_2 \simeq \frac{C_2}{Q^6} \quad (3)$$

where the numbers C_1 and C_2 are determined by the wave functions. Explicit PQCD calculations⁴ give

$$G_M^p = \frac{\alpha_s^2(Q^2)}{Q^4} \sum_{n,m} d_{nm} \left(\ln \frac{Q^2}{\Lambda^2}\right)^{-\gamma_m - \gamma_n} \quad (4)$$

If G_M^p falls like $1/Q^4$ at large Q^2 , this could be evidence that PQCD is working and scattering from the three valence quarks determines the form factor. There is also a smaller logarithmic dependence on Q^2 contained in the factor $\alpha_s^2(Q^2)$ and in the factors d_{nm} from the quark wave functions.

The early hope was that the wave function dependence would be small allowing a clean test of PQCD. The factor $\alpha_S^2(Q^2)$ could cause G_M^p to decrease faster than $1/Q^4$, with the amount depending on the size of Λ_{QCD} , and give direct evidence for the running of the coupling constant. Recently that hope has been questioned,⁶ and the role of the wave functions has been vigorously investigated⁷⁻⁹

New Data for ep Scattering

A new experiment¹⁰ on ep elastic scattering at large Q^2 was recently performed at SLAC to obtain high quality data at large Q^2 to measure the slope of G_M^p versus Q^2 . The high current SLAC beam up to 20 GeV and a 60 cm long liquid hydrogen target and the 8 GeV/c spectrometer were used to measure from

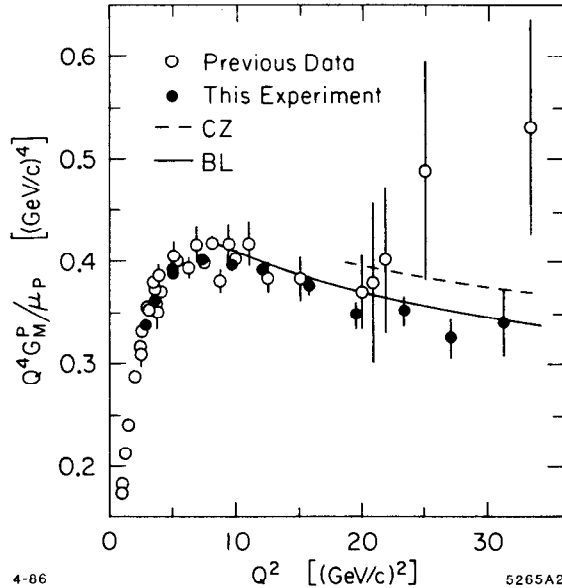


Fig. 1. New results for the proton form factor G_M^p from Ref. 10. The perturbative QCD curves are: BL (Ref. 4), CZ (Ref. 7).

and also give fair agreement with the size and shape for G_M^p . If this work survives further tests, it could lead to the rather surprising conclusion that the valence quarks in a nucleon do not more or less equally share the momentum. If this were true it would have important consequences in other areas of physics.

The Neutron

One place to test these questions is in the data for the neutron form factors. For convenience we discuss the neutron in terms of the ratio to the proton. The ratio is also useful for comparison to some calculations because many factors

$Q^2 = 2.9$ to 31.3 $(\text{GeV}/c)^2$ (Fig. 1). The results show $Q^4 G_M^p$ attaining a constant value between 5 and 12 $(\text{GeV}/c)^2$ and then slowly decreasing with increasing Q^2 . This shape is consistent with the predictions of PQCD, but this interpretation must be made with some caution.

The first PQCD calculations⁴ used symmetric wave functions (all quarks have equal probability for carrying some fraction x of the proton momentum). It turns out that the lowest order PQCD diagrams are exactly zero for symmetric wave functions. Chernyak and Zhitnitsky⁷ have derived a set of asymmetric wave functions which satisfy the constraints from QCD sum rules

affecting the normalizations cancel. Recall that for small scattering angles where the terms in the cross section proportional to $\tan^2(\theta/2)$ are small,

$$\frac{\sigma_n}{\sigma_p} = \frac{F_{1n}^2 + \frac{Q^2}{4m^2} F_{2n}^2}{F_{1p}^2 + \frac{Q^2}{4m^2} F_{2p}^2}. \quad (5)$$

Several possibilities can be considered. If F_{1n} is zero, or small compared to F_{2n} , which would happen if the nucleon wave function were spatially symmetric, then σ_n would be due only to the higher order term F_{2n} . At large Q^2 the ratio would become

$$\frac{\sigma_n}{\sigma_p} \Rightarrow \left(\frac{C_{2n}}{C_{1p}} \right)^2 \frac{4m}{Q^2} \quad (6)$$

and decrease with increasing Q^2 . If F_{1n} is comparable to F_{2n} , then σ_n would eventually be due to F_{1n} at large Q^2 , and the ratio σ_n/σ_p would be some number determined by the wave functions

$$\frac{\sigma_n}{\sigma_p} \Rightarrow \left(\frac{C_{1n}}{C_{1p}} \right)^2. \quad (7)$$

If the struck quark has the same flavor as the nucleon (u for the proton, d for the neutron), then $\sigma_n/\sigma_p \rightarrow 1/4$; if the struck quark has the same helicity,

$$\sigma_n/\sigma_p \rightarrow 3/7.$$

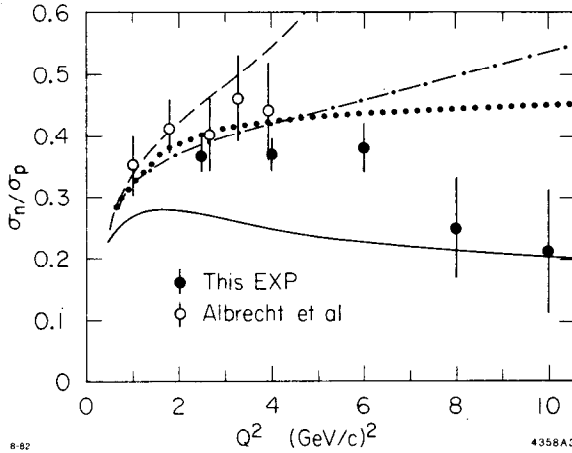


Fig. 2. The ratio of elastic neutron and proton cross sections, data from Ref 11. The dashed and solid curves are from VMD models by Höhler et al and Blatnik and Zovko (Ref. 1). The dotted curve is form factor scaling: $G_M^n/\mu_n = G_M^p/\mu_p = G_E^p$ and $G_E^n = 0$. The dashed-dot curve is the dipole law for G_M^n with $G_E^n = 0$.

The data¹¹ for σ_n/σ_p (Fig. 2) shows a nearly constant value from 1 to 6 $(\text{GeV}/c)^2$ and then a decrease at higher Q^2 . This shape is consistent either with $F_{1n} \simeq 0$, or $F_{1n} \neq 0$ and the same flavor for the struck quarks.

A recent theoretical development that may provide some guidance for interpreting the form factor data comes from Gari and Krümpelmann.¹² They have constructed a phenomenological merger of a VMD model with the asymptotic constraints from QCD. The usual VMD expressions¹ for nucleon form factors (without ϕ mesons) are augmented with a momentum

dependent factor containing a new scale parameter Λ_2 . The meson-nucleon and the Pauli and Dirac e.m. form factors are written as

$$F_1 = \frac{\Lambda_1^2}{\Lambda_1^2 + \hat{Q}^2} \frac{\Lambda_2^2}{\Lambda_2^2 + \hat{Q}^2} \quad (8.a)$$

$$F_2 = F_1 \frac{\Lambda_2^2}{\Lambda_2^2 + \hat{Q}^2}. \quad (8.b)$$

The value of $\Lambda_1 = 0.8$ GeV is determined from meson nucleon coupling; the effective momentum transfer \hat{Q}^2 contains the logarithmic variation $\log(Q^2/\Lambda_{QCD}^2)$. The parameter Λ_2 , to be determined from fits to the form factor data, adjusts the transition from VMD to QCD. For $Q^2 \ll \Lambda_2^2$ the momentum dependence follows the monopole form factors F_1 and F_2 plus the vector meson propagators. For $Q^2 \gg \Lambda_2^2$ the meson propagators die away and $F_1 \sim 1/Q^4$ while $F_2 \sim 1/Q^6$.

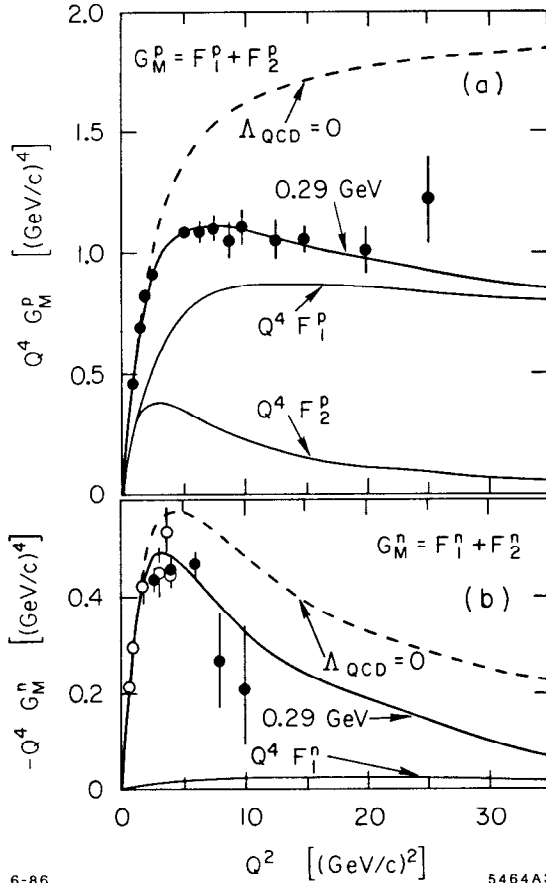


Fig. 3. Results from the VMD + QCD model of Ref. 12. a) the proton G_M^p , b) the neutron G_M^n .

Gari and Krümpelmann fit their model simultaneously to all the available nucleon form factor data (results from Ref. 10 not included). At large Q^2 the G_M^p is mostly due to F_{1p} (Fig. 3a). However, F_{2p} makes a substantial contribution, and we have to be careful when comparing the data to calculations which do not include F_2 . The available perturbative QCD calculations^{4,7} are ambiguous on this point. They calculate G_M^p , which is identical with F_{1p} asymptotically. No perturbative calculation of F_{2p} has been done.

The situation for G_M^n is quite different (Fig. 3b). In the Gari and Krümpelmann model F_{1n} is small, near zero, compared to F_{2n} . This result follows from the near cancelation of terms from ρ and ω mesons, and is driven by the requirement to fit the high Q^2 data for σ_n/σ_p in Fig. 2. This phenomenological model could be providing

the clues that we need to answer key questions. The value of $\Lambda_2^2 = 5.15 \text{ GeV}^2$ indicates the transition to the perturbative regime may take place around $5 (\text{GeV}/c)^2$. The value $\Delta_{QCD} = 0.29 \text{ GeV}$ is consistent with results determined from scaling violations in deep inelastic scattering.¹³ The problem remains how to understand the relative magnitudes of F_1 and F_2 determined by the quark wave functions.

The consequences of $F_{1n} \simeq 0$ are several:

a) From the definition Eq. (1) it follows that G_E^n and G_M^n will be comparable in size around $Q^2 = 4 (\text{GeV}/c)^2$ (Fig. 4). It could be that the folklore that G_E^n is small, maybe zero, is true at low Q^2 , but at higher Q^2 the situation is completely reversed (Fig. 4). This prediction can be tested in a standard Rosenbluth measurement of quasielastic ed scattering.¹⁴

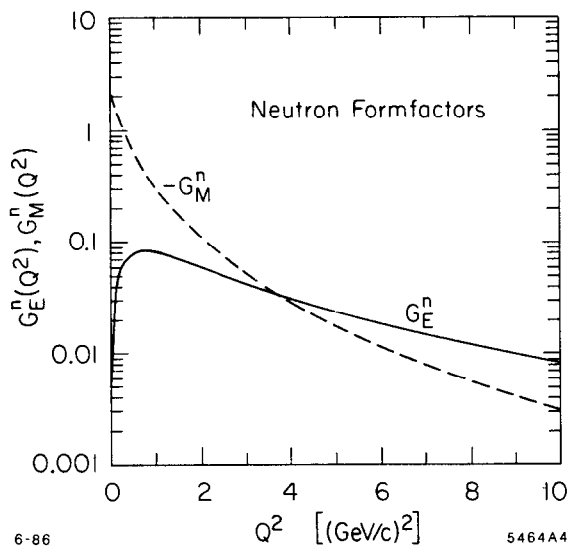


Fig. 4. The neutron form factors G_E^n and G_M^n from Ref. 12.

b) σ_n is determined by the higher order helicity flip term F_2^n and it does not make sense to compare first order PQCD results to the neutron data. The neutron cross section at high Q^2 may provide a useful testing ground for the higher order terms.

c) Knowledge of the neutron form factors is essential for interpretation of other electromagnetic data. One key example is the deuteron forward angle elastic form factor $A(Q^2)$, which in the impulse approximation is mostly proportional to the isoscalar charge form factor

$$A \sim (G_E^p + G_E^n)^2 \phi_{body}^2. \quad (9)$$

The smaller G_E^n beats against the larger G_E^p and small changes around zero give big effects in $A(Q^2)$. It is possible that a long standing inability of the impulse calculations¹⁵ to give large enough values for $A(Q^2)$ could be traced to using the wrong neutron form factor (Fig. 5).

THE DEUTERON

Measurements of the deuteron form factors at large Q^2 provide important tests of reaction mechanisms and the nature of the nucleon constituents at short distance. The deuteron magnetic form factor $B(Q^2)$ is expected to be especially sensitive to ingredients in the description.¹⁶⁻¹⁹ There is now available

very preliminary data from a new experiment²⁰ at SLAC, with data taking still underway at the time of this conference. The previous data²¹ and examples of the range of predictions are shown in Fig. 6. The $B(Q^2)$ is expected to be small compared to $A(Q^2)$ and therefore measurements at large angles are necessary. The new experiment measured ed scattering in coincidence around 180 degrees. The calculations range from impulse models¹⁵⁻¹⁷ which all predict sharp diffraction features, to quark scaling predictions^{4,18} with smooth power law fall off. Some models also include scattering from meson exchange currents,¹⁷ delta components in the wave function, or 6-quark components at the core of the wave function.¹⁹ These mechanisms can shift or in some cases totally obliterate the diffraction features from the impulse approximation.

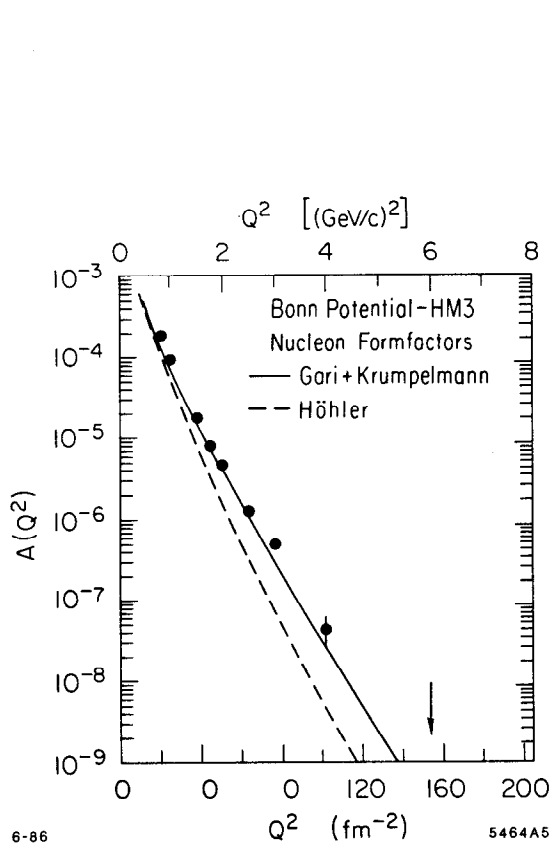


Fig. 5. Comparison of impulse approximation calculations (Ref. 15) for the deuteron $A(Q^2)$ using nucleon form factors from Refs. 1 and 12.

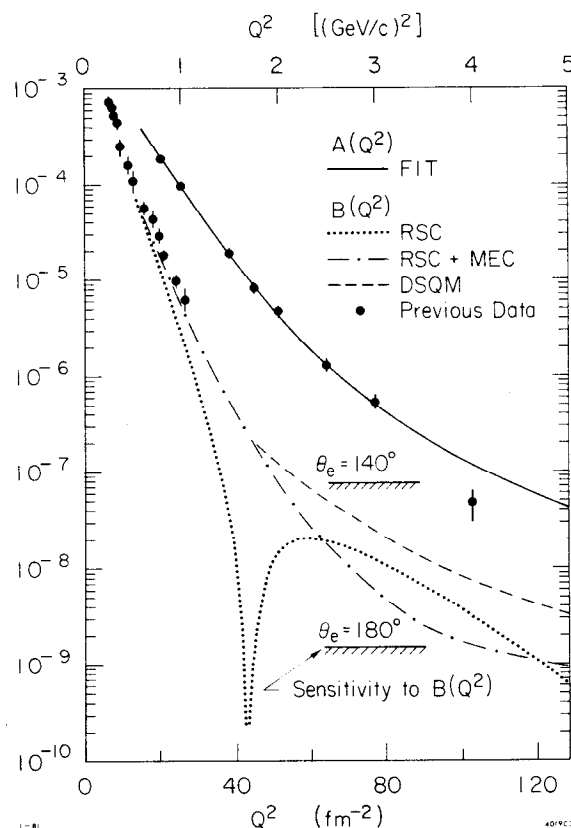


Fig. 6. Deuteron form factors $A(Q^2)$ and $B(Q^2)$. The curves for $B(Q^2)$ are impulse approximation calculations using reid soft core wave functions, with and without meson exchange currents (Ref. 17) and the dimensional scaling quark model (Ref. 3), arbitrarily normalized at $Q^2 = 1.75 (\text{GeV}/c)^2$.

The new data (Fig. 7) fall very quickly with Q^2 and seem to indicate a deviation from a smooth decrease around 2 to 2.5 $(\text{GeV}/c)^2$. The cross sections at high Q^2 are very low ($\sim 10^{-42} \text{ cm}^2/\text{sr}$), leading to counting rates of events

per week. This new data nearly doubles the range in measured Q^2 and will help narrow the choices for short range deuteron structure.

TRITIUM

Two recent experiments, one at Saclay,²² and one at MIT-Bates,²³ have given a large increase in the experimental information on tritium e.m. structure. These are the long awaited results of major efforts to build difficult liquid²² and gaseous²³ tritium targets for use in high powered electron beams. The Saclay experiment measured elastic scattering. The charge and magnetic form factors were separated

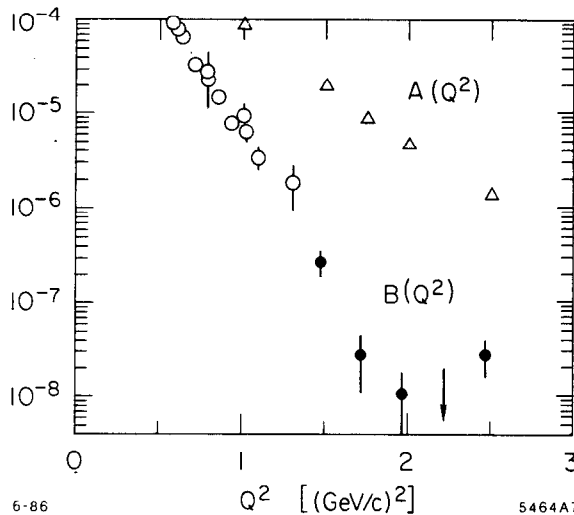


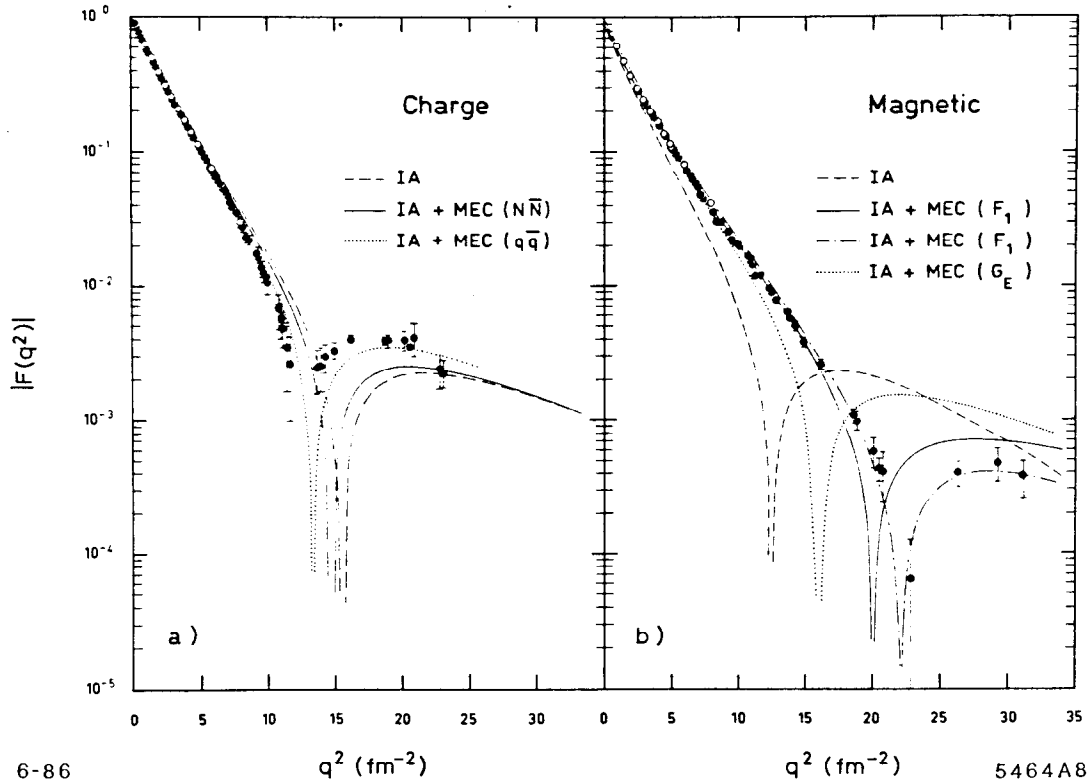
Fig. 7. Preliminary results for $B(Q^2)$ (Ref. 20) and previous data (Ref. 21).

out to Q^2 around 1 $(\text{GeV}/c)^2$ and the diffraction features in each have now been revealed (Fig. 8). This data, taken together with similar data already available for ^3He , will provide important information needed to sort out the three-body wave functions, the role of meson currents, isobar contributions, and off-shell nucleon form factors. As Figure 8 shows, F_{mag} is particularly sensitive to the meson currents and the choice of nucleon form factors.

The MIT-Bates experiment,²³ which completed data taking only a few weeks ago, was optimized for careful comparison of inelastic scattering from ^3He and ^3H . Extensive data were obtained for longitudinal and transverse separations in the quasielastic and delta excitation region over the kinematic range accessible with 700 MeV beam (Fig. 9). This data provides a high quality look at the inelastic response function in the lightest nuclei where explicit multi-nucleon effects can appear. The MIT-Bates experiment also measured three points on the charge form factor at Q^2 around 1 $(\text{GeV}/c)^2$ that confirm the Saclay results and extends the Q^2 range slightly.

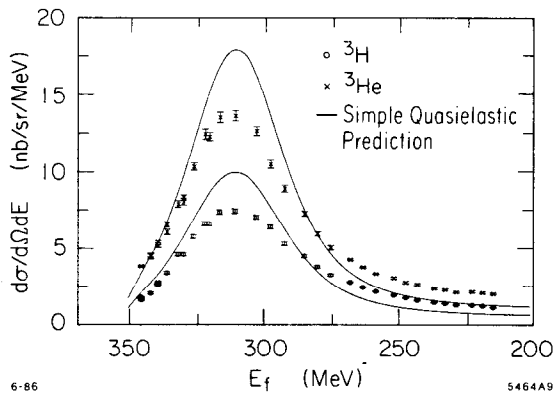
QUASIELASTIC SCATTERING — γ -SCALING

Inelastic electron scattering from nuclei in the kinematic region of quasi-free scattering on bound nucleons has attracted a lot of attention recently. The main interest stems from the suggestion by West²⁷ that such data might be interpreted to yield universal momentum distributions for nucleons in nuclei.



6-86 5464A8
 Fig. 8. Results for the tritium charge and magnetic form factors from Saclay (Ref. 22). The theoretical curves are impulse approximation models, some with meson exchange currents, and for various nucleon form factors (Refs. 25 and 26).

The scattering mechanism in this region of the response function is pictured to be quasi-free knockout of single nucleons. The chance for scattering is factorized into a probability $F(y)$ for finding nucleons with mass m moving at momentum y in the initial nucleus, times the cross section for e-nucleon scattering assuming the same form factors as for free nucleons. The $F(y)$ can be deduced from the experimental cross section using



6-86 5464A9
 Fig. 9. Preliminary results for quasielastic electron scattering from ^3H and ^3He from MIT-Bates (Ref. 23).

$F(y) = \frac{\left(\frac{d\sigma}{d\Omega dE'}\right)_{exp} dE'}{\left[Z\frac{d\sigma}{d\Omega} + N\frac{d\sigma}{d\Omega}\right] dy} \quad (10)$

where y is obtained from energy and momentum conservation

$$E = E' - \bar{\epsilon} + \sqrt{(\vec{p} + \vec{q})^2 + m^2} - m + \sqrt{p^2 + (A-1)^2 m^2} - (A-1)m. \quad (11)$$

Various approximations and assumptions are usually applied to the scaling analysis. In most formulations^{28,29} for large Q^2 the initial nucleon transverse momentum k_{\perp} is ignored and then y can be identified with the component of \vec{k} parallel to \vec{q} . This approximation also simplifies the kinematical factor dE'/dy which can affect the way the data scale.³⁰

Another problem is what to do about the final state interaction of the knocked out nucleon with the $(A-1)$ system and the excitations of the residual nucleus. The term $\bar{\epsilon}$ in Eq. (11), representing an average nucleon separation energy, has sometimes been included²⁸ to approximately account for these effects for analysis of data for the light nuclei (^3He), but this may not be adequate for heavier nuclei.³¹ There is also some question about whether it is safe to assume that bound nucleons have the same form factors as free ones, especially at large y (sometimes as large as 600 to 800 MeV/c), where the nucleons are clearly strongly interacting with their neighbors.

Notwithstanding these questions, the y -scaling analysis provides an important method for synthesizing large amounts of data. By virtue of the fact that it works (ie. the data scale), it leads people to accept the basic assumption of single nucleon knockout and continue to regard the derived $F(y)$ as a source of information about the high momentum components.

Preliminary results were presented at this conference from a new experiment³² that measured quasielastic scattering from a series of nuclei at forward angles (15° to 30°) and beam energies from 2 to 3.6 GeV, corresponding to momentum transfer in the range 0.2 to 2.2 $(\text{GeV}/c)^2$.

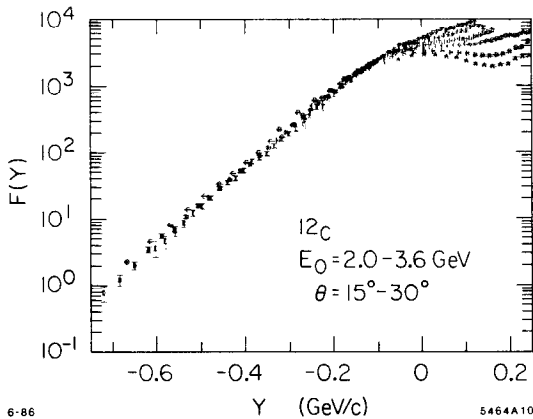


Fig. 10. Preliminary results for quasielastic electron scattering from ^{12}C (Ref. 32).

An example of one series of spectra for ^{12}C is shown in Fig. 10. The original data spanning six orders of magnitude in the cross section are reduced to a universal scaling function in the region of negative y . Comparing similar data for nuclei throughout the periodic table will give insight into the nuclear dependence of the scaling hypothesis.

There presently exists a puzzle in quasielastic scattering which could be giving hints of important new physics. When quasielastic data³³ taken at various angles are analyzed³⁴ to give separate longitudinal and transverse response

functions, there is a large difference between the $F(y)$ for longitudinal and transverse scattering even at the quasielastic peak. The ratio of longitudinal to transverse response for ^{56}Fe is about 0.55, for example. This result contradicts the basic assumption that there should be a universal $F(y)$ for each nucleus.

One suggestion is that these results are obtained because the wrong (free) nucleon form factors were used in the analysis, and that perhaps this effect is another manifestation of modified (swollen) nucleons that is seen also in the EMC effect. To advance the study of this problem, a new experiment³⁵ is being prepared at SLAC to extend the longitudinal-transverse separation for several nuclei out to Q^2 around 1 $(\text{GeV}/c)^2$.

In a related area of physics, two recent experiments³⁶ measured inelastic scattering in the nucleon resonance region at Q^2 below 1 $(\text{GeV}/c)^2$ to study the nuclear dependence of delta excitation.

DEEP INELASTIC SCATTERING — THE EMC EFFECT

The discovery³⁷ by the European Muon Collaboration that deep inelastic scattering per nucleon from iron was not the same as for deuterium is widely regarded as an important signature for the modification of the quark distributions for bound nucleons. Subsequent data³⁸ from SLAC agreed with the EMC for $x > 0.3$ and showed that the effect increases with A proportional to the average nuclear density. There remained a discrepancy between EMC and SLAC data for x below 0.3 (Fig. 11).

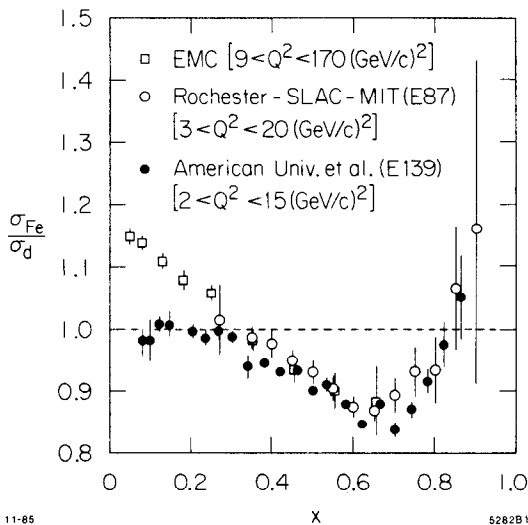
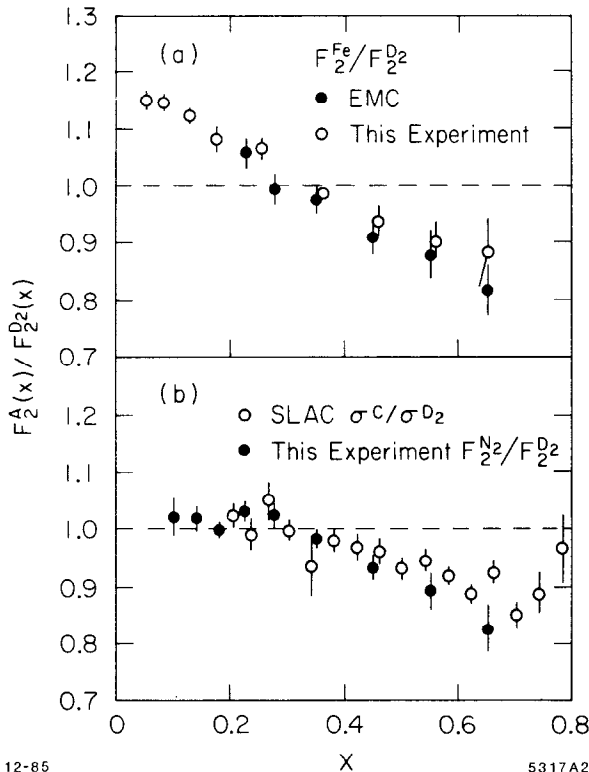


Fig. 11. The ratio of deep inelastic muon and electron cross sections for iron and deuterium from EMC (Ref. 37) and SLAC (Ref. 38).

The suggested explanations for the EMC effect have been many,³⁹ but most ascribe it to a softening (shift to lower momentum) of the valence quark distribution for bound nucleons, accompanied by an increase in the momentum carried by ocean quarks at low x . This phenomenon can be viewed as caused by an effective increase in the confinement radius for the quarks in bound nucleons, either by nucleon swelling, overlap into clusters, creation of extra pions, or excited nucleons. The region of x below 0.3 is expected to contain complex physics in which shadowing of the virtual photons competes with scattering from pointlike

quarks or clusters of quarks (higher twist terms in PQCD) to give effects varying with x , Q^2 , A , and ϵ (the virtual photon polarization). The large discrepancy between EMC and SLAC data at low x has helped fuel this discussion, and has stimulated models⁴⁰ which depend on enhanced pion content at low x for redistribution of the momentum.

A new measurement⁴¹ by the BCDMS collaboration at CERN of muon scattering on nitrogen and iron has confirmed the effect for $x > 0.3$ (Fig. 12). They only have data at lower x for nitrogen which agree with the trend of the SLAC data.



12-85

5317A2

Fig. 12. (a) The ratio of the structure functions F_2 for iron and deuterium as measured by BCDMS (Ref. 41) and EMC (Ref. 37). (b) BCDMS nitrogen data compared to SLAC data (Ref. 38) for carbon. Only statistical errors are shown.

It is conceivable that part of the discrepancy between EMC and SLAC could be due to a difference for $R = \sigma_L / \sigma_T$ for heavy nuclei compared to deuterium.⁴² This might be caused, for example, by more higher twist contributions from spin-zero components in nuclei (diquarks or quasi pions) that generates a larger σ_L . The EMC measures near $\epsilon = 1$ and their cross sections are mostly due to $F_2(x, Q^2)$, whereas the SLAC data are measured at ϵ in the range 0.4 to 0.9. Extraction of $F_2(x, Q^2)$ from the cross sections is sensitive to R . A new SLAC experiment⁴³ has measured R for deuterium, Fe, and Au at $x = 0.2, 0.35, 0.5$; when results are available they should help settle this question.

Meanwhile new important results⁴⁴ from the EMC have been presented at this conference which indicate the EMC effect may not be as large at low x as previously thought. Data were taken in such

a way as to reduce many of the systematic errors from uncertainty in the acceptance by measuring with different targets (d, He, C, Cu, Sn) in the same geometry. Preliminary results from a partial data sample for Cu (Fig. 13) show a ratio $\sigma_{\text{Cu}} / \sigma_{\text{d}}$ at low x which never goes above 1.1 and falls to less than one at x below 0.1. The new EMC data are within errors of the SLAC data, though

there are small deviations that could be due to variations with Q^2 or ϵ that needs to be sorted out. The large rise at small x in the original EMC data is apparently not real. The new EMC data are consistent with the original values when the systematic errors are included.

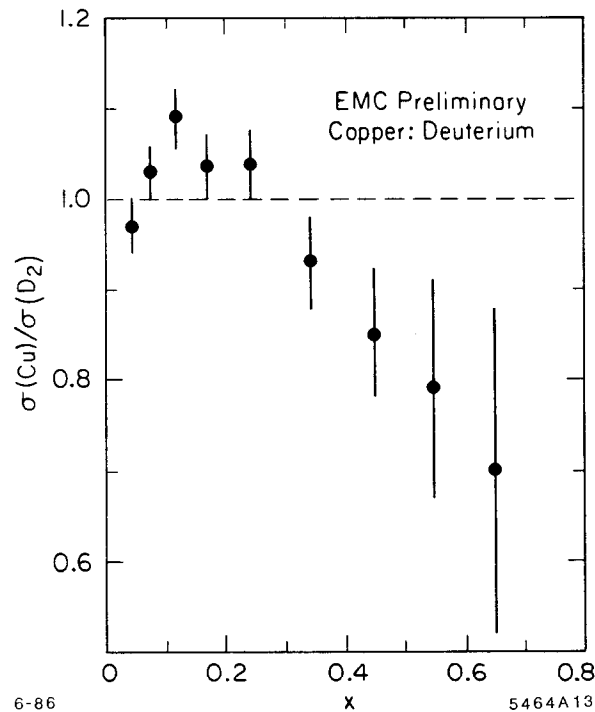


Fig. 13. Preliminary results for the ratio of muon scattering cross sections for Cu and d (Ref. 44).

FUTURE PROSPECTS

A new experiment⁴⁵ measuring inclusive muon scattering at CERN using an improved EMC apparatus will begin data taking soon. This experiment will yield high statistics data for a series of nuclei that will be extremely useful for understanding the physics in the low x region. An experiment⁴⁶ is being prepared at Fermilab to measure muon scattering using the new high energy beam from the Tevetron. This experiment will complement the CERN efforts by concentrating on measurements of the final state. Possibilities for internal target experiments at the PEP storage ring at SLAC are now being investigated⁴⁷. This could lead to a new generation of electromagnetic probes of nucleon and nuclear targets at GeV energies measuring multiparticle final states, perhaps with polarized beams and targets.

REFERENCES

1. G. Höhler et al., Nucl. Phys. B114, 505(1976); S. Blatnik, N. Zovko, Acta Phys. Austriaca 39, 62(1974), F. Iachello, A. Jackson, A. Lande, Phys. Lett. 43B, 191(1973).
2. S. Brodsky, G. Farrar, Phys. Rev. D11, 1309(1975).
3. S. Brodsky, B. Chertok, Phys. Rev. D14, 3003(1976).
4. S. Brodsky, G. Lepage, Phys. Rev. D22, 2157(1980).
5. G. Farrar, D. Jackson, Phys. Rev. Lett. 35, 1416(1975); I. A. Vainshtein, V. I. Zakharov, Phys. Lett. 72B, 368(1978).
6. N. Isgur, C. Llewellyn Smith, Phys. Rev. Lett. 52, 1080(1984).
7. V. L. Chernyak, I. R. Zhitnitsky, Nucl. Phys. B246, 52(1984), V. L. Chernyak, A. R. Zhitnitsky, Phys. Rep. 112, 173(1984).
8. C. Carlson, Proceedings of the Nato Advanced Study Inst., Banff, Canada, Aug 22 - Sept 4 1985.
9. M. Gari, N. G. Stefanis, Ruhr Universität Bochum Print RUB TPII-85-16; RUB TPII-85-23 (1986).
10. R. Arnold et al., SLAC PUB 3810 (1986); Phys. Rev. Lett. 57, 174(1986).
11. S. Rock et al., Phys. Rev. Lett. 49, 1139(1982); R. J. Budnitz et al., Phys. Rev. 173, 1357(1968); W. Albrecht et al., Phys. Rev. 26B, 642(1968).
12. M. Gari, W. Krümpelmann, Z. Phys. A322, 689(1986); Ruhr Universität Bochum Print RUB TPII-86-5 (1986).
13. J. J. Aubert et al., Phys. Lett. 114B, 291(1982).
14. R. Arnold et al., "A Proposal to Separate the Charge and Magnetic Form Factors of the Neutron at Momentum Transfer $Q^2 = 2$ to $5 Q^2$ ", SLAC-NPAS Proposal NE11 (1986).
15. Examples of impulse approximation results for deuteron form factors including relativistic effects are given in R. Arnold, C. Carlson, F. Gross, Phys. Rev. C21, 1426(1980). The effect of assuming $F_{1n} = 0$ was noted.
16. R. S. Bhalerao, S. A. Gurvitz, Phys. Rev. Lett. 47, 1815(1981).
17. M. Gari, G. Hyuga, Nucl. Phys. A264, 409(1976), Nucl. Phys. A278, 372(1977).
18. S. Brodsky, C. Ji, G. P. Lepage, Phys. Rev. Lett. 51, 83(1983).
19. A. P. Kobushkin, V. P. Shelest, Sov. J. Part. Nucl. Phys. 14, 483(1983).
20. P. Bosted, this conference, preliminary results of SLAC-NPAS experiment NE4, "Measurements of electron deuteron scattering at 180 degrees at large momentum transfer."

21. S. Auffret, et al., Phys. Rev. Lett. 54, 649(1985); R. Cramer, et al., Z. Phys. C29, 513(1985).
22. F. P. Juster et al., Phys. Rev. Lett. 55, 2261(1985).
23. B. Beck, this conference, preliminary results of elastic and inelastic electron scattering from ^3H and ^3He at MIT-Bates.
24. R. Arnold et al., Phys. Rev. Lett. 40, 1429(1978); J. M. Cavedon et al., Phys. Rev. Lett. 49(1982).
25. W. Strueve, C. Hajduk, P. U. Sauer, Nucl. Phys. A405, 620(1983); C. Hajduk, P. U. Sauer, W. Strueve, Nucl. Phys. A405, 581(1983); E. Hadjimichael, B. Goulard, R. Bornais, Phys. Rev. C27, 831(1983).
26. M. Beyer et al., Phys. Rev. Lett. 122B, 1(1983).
27. G. B. West, Phys. Rep. 18C, 263(1975).
28. I. Sick, D. Day, J. S. McCarthy, Phys. Rev. Lett. 45, 871(1980).
29. P. Bosted et al., Phys. Rev. Lett. 49, 1380(1982).
30. C. Ciofi degli Atti, E Pace, G. Salame INFN (Rome) Print INFN-ISS 85/7 (1985), to be published in Czech. J. Phys.
31. S. A. Gurvitz, J. A. Tjon, S. J. Wallace, U. Md Print 86-103(1986).
32. D. Day, this conference, preliminary results from SLAC-NPAS experiment NE3, "Inclusive electron scattering measurements from nuclei."
33. Z. Meziani et al., Phys. Rev. Lett. 52, 2130(1984); 54, 1237(1985).
34. Z. Meziani, SLAC PUB 3939 (1986).
35. Z. Meziani et al., SLAC-NPAS Proposal NE9 (1985),
36. S. Thornton et al., SLAC-NPAS Experiment NE1 (1985); H. Jackson et al., SLAC-NPAS Experiment NE5 (1985).
37. J. J. Aubert et al., Phys. Letters 123B, 275(1983).
38. A. Bodek et al., Phys. Rev. Lett. 50, 1431; 51, 534(1983); R. Arnold et al., Phys. Rev. Lett. 52, 727(1984).
39. N. N. Nikolaev, "EMC Effect and Quark Degrees of Freedom in Nuclei: Facts and Fancy", Oxford Print TP-58/84, Invited Talk at VII Int. Seminar on Problems of High Energy Physics–Multiquark Interactions and Quantum Chromodynamics, Dubna USSR, 19-23 June 1984; R. R. Norton, "The Experimental Status of the EMC Effect", Rutherford Print RAL-85-054, Topical Seminar on Few and Many Quark Systems, San Marino, Italy 25-29 March 1985; H. J. Pirner, "Deep Inelastic Lepton-Nucleus Scattering", Proc. Int. School of Nucl. Phys. Erice, to be pub. Progress in Particle and Nuclear Physics (1984); R. L. Jaffe, "The EMC effect today", Proc. Workshop on Nuclear Chromodynamics," Santa Barbara, Aug (1985), pub. by World Scientific.

40. E. L. Berger, F. Coester, Phys. Rev. D32, 1071(1985).
41. G. Bari et al., Phys. Lett. 163B, 282(1985).
42. S. Rock, 22nd Int. Conf. on High Energy Phy., Leipzig East Germany, July 19-25(1984); J. Gomez, SLAC PUB 3552(1985).
43. R. Arnold et al., SLAC Experiment E140, "Measurement of the x , Q^2 , and A-Dependence of R" (1985).
44. G. Taylor, this conference, preliminary results from the EMC (1986).
45. D. Allasia et al, the New Muon Collaboration (NMC), CERN Proposal SPSC/P210, "Detailed Measurements of Structure Functions from Nucleons and Nuclei", February 1985.
46. Fermilab experiment E665, T. B. Kirk, (FNAL), V. Eckardt (MPI) spokesmen; D. F. Geesaman, M. C. Green, Argonne print PHY-4622-ME-85 (1985).
47. F. Dietrich, this conference, results of a test experiment using a gas target in the PEP ring at SLAC.